Cellulose (2019) 26:5291–5303
https://doi.org/10.1007/s10570-019-02435-8

ORIGINAL RESEARCH

Highly temperature resistant cellulose nanofiber/polyvinyl alcohol hydrogel using aldehyde cellulose nanofiber as cross-linker

Longxiang Zhu · Yun Liu · Zhiming Jiang · Eiichi Sakai · Jianhui Qiu · Ping Zhu

Received: 17 September 2018 / Accepted: 15 April 2019 / Published online: 29 April 2019

Abstract Polyvinyl alcohol (PVA) based hydrogels, generally prepared by freeze–thaw methods, are commonly used in the field of wound dressing. Biomedical materials require rigorous sterilization prior to use which can result in the decomposition of hydrogen bonded PVA hydrogels during conventional high temperature sterilization. In this study, a highly temperature resistant cellulose nanofiber/polyvinyl alcohol (CNF/PVA) hydrogel is prepared using functionalized CNF as a chemical cross-linker. $NaIO_4$ is utilized to selectively oxidize CNF to increase CNF chemical reactivity. The crystallinity and the thermal decomposition temperature of CNF show a decreasing trend with the increase of oxidant content. The CNF/PVA hydrogels are synthesized with functional CNF and PVA at 80 °C under acidic condition through aldolization. The mechanical strength and modulus of the hydrogel (CNF-3/PVA) with more chemical cross-linking networks are 0.43 MPa and 0.25 MPa, respectively. The hydrogel exhibits a water content (82.7%) close to that of the organism tissue and not decompose or swell much during the high-temperature sterilization treatment. In addition, the produced hydrogel shows the same softening effect as living tissue.

Electronic supplementary material The online version of this article (https://doi.org/10.1007/s10570-019-02435-8) contains supplementary material, which is available to authorized users.

L. Zhu (✉) · Y. Liu · Z. Jiang · P. Zhu
Institute of Functional Textiles and Advanced Materials, College of Textiles and Clothing, Qingdao University, Qingdao 266071, China
e-mail: lxzhu@qdu.edu.cn

L. Zhu · E. Sakai · J. Qiu (✉)
Department of Machine Intelligence and Systems Engineering, Faculty of Systems Engineering, Akita Prefectural University, Akita 015-0055, Japan
e-mail: qiu@akita-pu.ac.jp

Graphical abstract

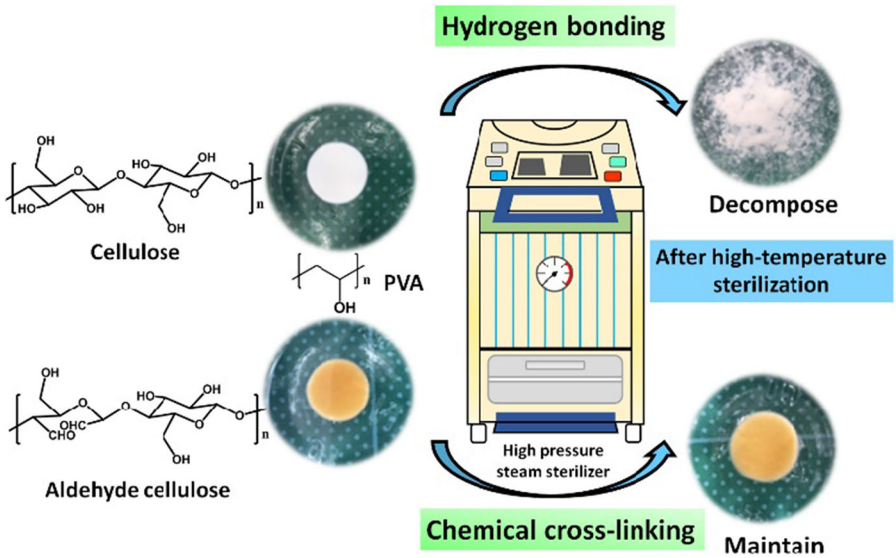

Keywords PVA hydrogel · Cellulose nanofiber · Macromolecule cross-linker · Mechanical properties · Thermal stability

Introduction

Soft and wet hydrogels usually are composed of three-dimensional polymer network structure and a large amount of water (50–99%) inside the network structure (Chen et al. 2015; Gong 2010). Hydrogels can usually be divided into natural polymer hydrogels, synthetic polymer hydrogels, and natural-synthetic polymer hydrogels. They are widely used in biomedical application due to their excellent biocompatibility and physical properties similar to natural tissue (Dong et al. 2016; Hoffman 2012; Qi et al. 2018; Slaughter et al. 2009).

Polyvinyl alcohol (PVA) is a synthetic linear polymer obtained from partial or full hydrolysis of polyvinyl acetate. The resulting PVA exhibits a high degree of water solubility, but is resistant to most organic solvents (Tubbs 1966). Due to its water solubility, it is usually necessary to introduce a cross-linking network in the PVA polymer solution to form a hydrogel for use in several applications. Strategies to prepare PVA hydrogel usually include irradiation (Peppas and Merrill 1976), cyclic freezing–thawing (Abitbol et al. 2011; Shi and Xiong 2013) and chemical reaction (Krumova et al. 2000; Mansur et al. 2008). PVA hydrogel is widely used as a commercial product in the biomedical field, such as for contact lenses (Karlgard et al. 2003; Kim et al. 2008), wound dressing (Elsner et al. 2011; Kamoun et al. 2017), and implantable medical materials (Chin et al. 2017), due to it bio-adhesive, non-toxic, biocompatible, and high chemical resistance (Baker et al. 2012).

Freeze–thaw technology is the most common cross-linking method for preparing PVA hydrogels (Abitbol et al. 2011). The molecular motion of the aqueous solution can be fixed by van der Waals forces and/or hydrogen bonds, and some molecular segments in a certain region can form an ordered structure. When re-freezing, more new ordered micro-domains are generated. These tightly combined ordered domains are no longer separated. The hydrogel established by this method has excellent mechanical strength at higher water content. Cellulose nanofiber (CNF), as natural material, possesses diverse characteristics different from conventional materials, including high specific surface area, rheological properties, liquid crystalline behavior, mechanical reinforcement, high surface chemical reactivity, biocompatibility, biodegradability, non-toxicity (Battirola et al. 2017; Klemm et al. 2011; Lin and Dufresne 2014; Zhang et al. 2017). On the basis of these unique properties, CNF has been

used in the biomedical field, for example, to improve the mechanical properties of PVA hydrogels for tissue engineering (Tummala et al. 2016a). This enhancement is typically achieved by hydrogen bonding of hydroxyl groups between CNF and PVA during hydrogel preparation (Tummala et al. 2016b, 2017; Yang et al. 2018). The reported positive cell toxicity studies have shown that CNF/PVA hydrogels provide a safe environment for cell growth (Tummala et al. 2016a). Besides, Tummala et al. (2017) reported that the tensile strength of CNF/PVA increased almost three-fold compared to the pure PVA hydrogel. However, CNF/PVA hydrogels formed by hydrogen bonding generally have thermal instability. Hydrogel as a biomedical material (e.g., wound dressing) requires severe sterilization before use. In our previous experiment, the PVA hydrogel prepared by freeze–thaw method was completely decomposed when using conventional autoclave sterilization. Since sterilization is an integral part of modern medical care, the thermal instability may be a defect of the synthesized PVA hydrogel with physical cross-linking. Chemical cross-linking of linear polymers provides feasible routes to improve mechanical properties and thermal stability (Mu et al. 2012; Ramaraj 2007). Therefore, a thermally stable PVA hydrogel can be produced by chemical cross-linking.

Conventional molecule cross-linkers can efficiently cross-link PVA. However, mechanical properties of the resulting product hydrogels are poor, and the potential toxicity of residual cross-linker molecules limits the application of hydrogels. In this work, CNF was used as cross-linker to prepare chemical cross-linking PVA hydrogel. First, to increase the reactivity of CNF, aldehyde cellulose nanofiber is prepared by using sodium periodate as the oxidant. Then, the modified cellulose is reacted with PVA at 80 °C under acidic condition through aldolization to obtain the hydrogel. Finally, the CNF/PVA hydrogel is reinforced through evaporation-swelling method according to our previous study (Zhu et al. 2017a). The oxidation degree of CNF has a significant effect on the activity of the acetal reaction, resulting in significantly different mechanical properties and water content of the hydrogel. The hydrogel shows exceptional thermal stability, which enhanced its application in the biomedical field, especially wound dressings.

Materials and methods

Materials

Cellulose nanofiber (CNF) purchased from Mori Machinery Corporation, Japan. Sodium periodate ($NaIO_4$) was obtained by Wako Pure Chemical Industries, Ltd., Japan. Polyvinyl alcohol (PVA) and Nitric acid (HNO_3) provided by Nacalai Tesque, Inc., Japan. All of the chemical reagents were used as-received. Distilled water was used in all experiments.

Oxidation of CNF

40 g CNF aqueous (5 wt% solid content) and 60 mL distilled water were added to 250 mL conical flask. The mixture was magnetically stirred for 10 min to disperse the CNF. Then a certain amount of $NaIO_4$ (12.5, 25, 37.5 and 50 wt%, $NaIO_4$ to CNF) was added into the conical flask, the mixture was magnetically stirred for 48 h under a dark environment. The oxidation products were separated by centrifugation (TOMY MX-305, 16,000 rpm (23,200 g), 12 min each time) and washing with distilled water for three times to remove the excess raw materials and reduce impurity. The number of the product is shown in Table 1.

Synthesis of the hydrogel

0.60 g of the oxide-CNF (CNF-1, CNF-2, CNF-3 and CNF-4) and 2 g PVA were dispersed into 30 mL water. The mixture was magnetically stirred for 1 h at 95 °C to ensure that the PVA dissolved completely and the CNF homogeneous dispersed. 5 drops of 0.5 M HNO_3 were added as a catalyst to the mixture after it was cooled to 60 °C. The hydrogel precursor was transferred into a sealed transparent mold after it

Table 1 The oxidation condition of CNF

	CNF[a] (g)	$NaIO_4$ (g)	H_2O (mL)
CNF-1	2	0.25	60
CNF-2	2	0.50	60
CNF-3	2	0.75	60
CNF-4	2	1.00	60

[a]The weight of CNF is the solid content

was stirred for 10 min. Finally, the mold was placed in an oven at 80 °C for 24 h. As a comparison, CNF/PVA having the same components with CNF-3/PVA also be prepared.

The evaporation–swelling (E–S) method was used to reinforce the mechanical performance of the hydrogel. In brief, the hydrogel was evaporation at 40 °C in an electrical blast drying oven for 24 h. After that, the CNF/PVA hydrogel was obtained after the dried hydrogel was swollen in distilled water for 60 h.

At last, the treated-hydrogels by E–S method were placed in an open glass vial and tested for high temperature resistance using a commercial high pressure steam sterilizer (TOMY, LSX-300). The high pressure steam system was held at 121 °C for 30 min.

Characterizations

A Thermo Scientific Nicolet iN 10 infrared spectrometer was used for the analysis of FT-IR. The sample was measured in the range of 650–4000 cm^{-1} with a resolution of 4 cm^{-1}. Both KBr pellet and ATR technique were adopted in the test. A total of 32 scans were accumulated.

The crystallographic structure of samples was obtained by X-ray diffraction system with a diffractometer (XRD 6000, Shimadzu Corporation, Japan) in range of 5–90° by step scanning. Nickel-filter Cu Kα radiation (λ = 0.15417 nm) was used with a generator voltage of 40 kV and a current of 30 mA.

Thermogravimetric analysis (TGA) and differential thermal analysis (DTA) of the samples were performed with TG instrument (DTG-60, Shimadzu Co., Ltd., Kyoto, Japan) at a scan rate of 10 °C min^{-1} from room temperature to 600 °C in N_2 atmosphere (flow rate of 50 mL/min). Sample (4–6 mg) were placed in aluminum crucibles by using an empty aluminum crucible as a reference. All of the samples were obtained from freeze-drying.

The morphologies of samples were characterized by SEM (S-4300, Hitachi Co., Ltd., Tokyo, Japan). Both CNF and CNF/PVA hydrogel samples were prepared through freeze-drying method. The sample was sputter-coated by gold with Ion sputter (E-1030, Hitachi Co., Ltd., Tokyo, Japan) for 3 or 5 min to provide enhanced conductivity before the test. The test voltage was 3 or 5 kV, and electric current was 10 μA.

The uniaxial elongation properties were carried out on a universal testing machine (Instron 3350 series, 50 N load cell, Instron Co., Ltd., Canton, America) and the measurement conditions were as follows: hydrogels were cut into the rectangle with the size of length 50 mm (l), gauge length 30 mm (l_o), width 10 mm (w) and height 0.5–1 mm (h), and tests were conducted at a cross-head speed of 500 mm/min. The cyclic compressive properties were measured using the same universal testing machine at a cross-head speed of 1 mm/min. Hydrogels were cut into disc shapes with a diameter 9 mm and height of 2.5 mm.

Results and discussions

Oxidation of CNF

Sodium periodate has a high selectivity for the oxidation of cellulose. This reaction breaks the C2–C3 bond of the glucopyranoside ring and produces two aldehyde groups at the C2 and C3 positions (Scheme 1a) (Kim et al. 2004; French 2017). The oxidation of CNF was carried out in a dark surrounding to prevent the degradation of $NaIO_4$, and the oxidation time was chosen to be 48 h to achieve a higher degree of oxidation. FT-IR spectra show that the peak intensities at 1060 cm^{-1} and 1130 cm^{-1} gradually decrease, indicating that the amount of hydroxyl groups in CNF decreases with increasing the $NaIO_4$ content. In addition, the peak at 1160 cm^{-1} is the stretching vibration of C2–C3, and the peak intensity decreases gradually, indicating that more C2–C3 bonds are oxidized when the number of oxidant molecules increases (Fig. 1a) (Dash et al. 2013). The increase of $NaIO_4$ during the oxidation process of CNF resulted in a corresponding increase in carbonyl content. As shown in Fig. 1b, the stretching vibration peak at 1730 cm^{-1} confirms the aldehyde is formed on the cellulose surface.

As illustrated in Fig. 2a, the crystallographic diffraction peaks of CNF at about 2θ = 22.7° for the (200) plane, 34.5° for the (004) plane gradually weakened with the increase of $NaIO_4$ content (French 2014). The crystallinity of the oxidized CNF is calculated according to Segal method (Thygesen et al. 2005), the equation as follows:

$$x_{CR}\% = \frac{I_{200} - I_{AM}}{I_{200}} \times 100\% \quad (1)$$

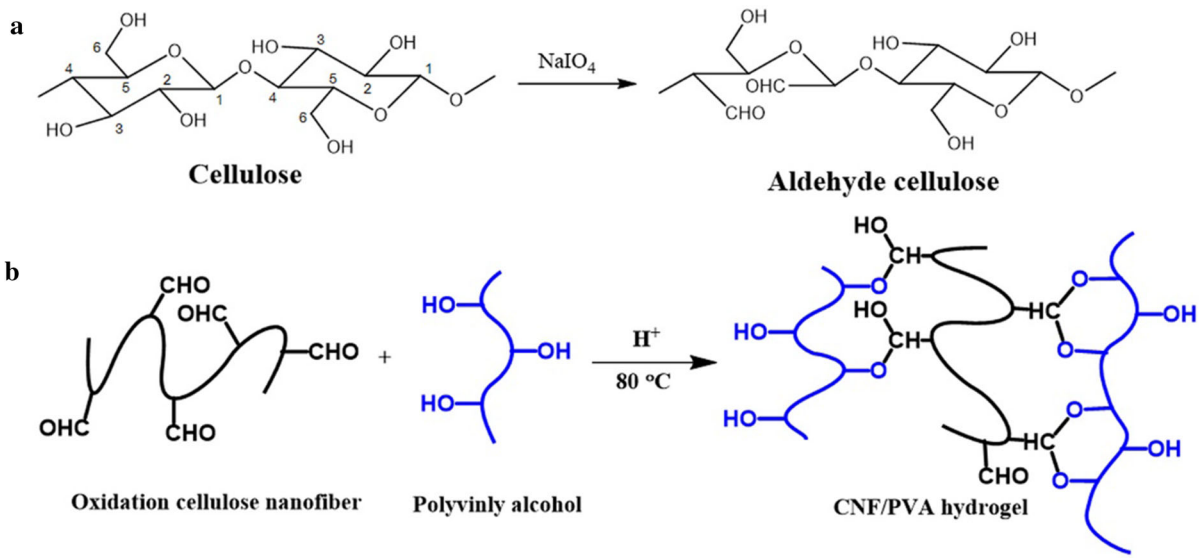

Scheme 1 **a** Schematic of cellulose nanofiber oxidation. **b** Gelation process of PVA and aldehyde cellulose by aldolization

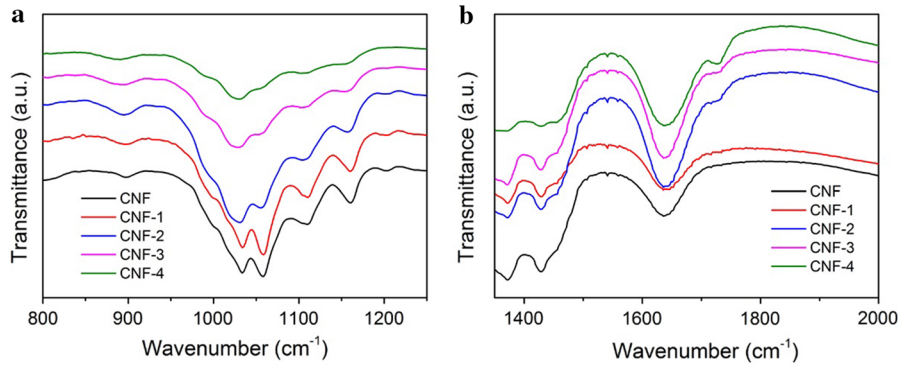

Fig. 1 FT-IR spectra of CNF and oxidized CNF. **a** Characterized by ATR. **b** Characterized by KBr pellet

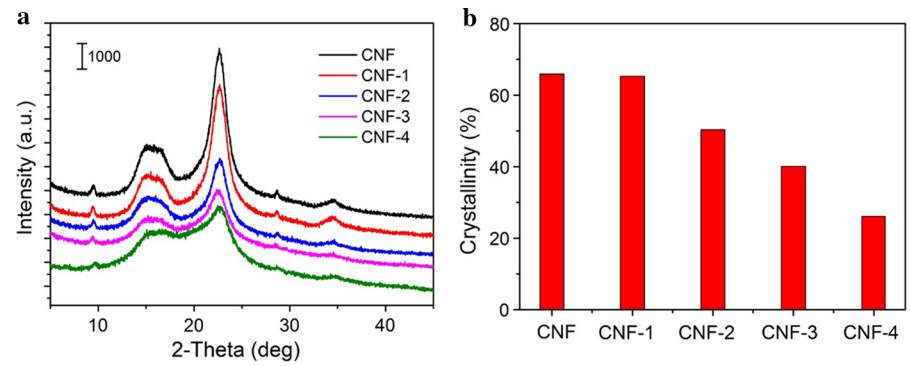

Fig. 2 **a** XRD of CNF and oxidation CNF. **b** The crystallinity of CNF and oxidized CNF

where I_{200} represents the crystalline and amorphous region, I_{AM} is the minimum between the 200 and 110 peak, and only represents the amorphous region. The crystallinity of CNF-1 has only a slight change (from 65.9 to 65.3%) compared with that of CNF in the case of lower $NaIO_4$ content (Fig. 2b). However, with more

$NaIO_4$ the crystallinity sharply decreased from 65.3 to 26.1%. The decrease in crystallinity of the oxidized CNF was explained by the fact that the structure and functional groups of the cellulose after oxidation were changed, resulting in a decrease in intramolecular and intermolecular hydrogen bonding of the cellulose.

Thermal properties of oxidation CNF

The thermal stability of CNF and oxidized CNF were evaluated by TGA (Fig. 3). A significant weight loss is observed at about 90–120 °C in the CNF and oxidized CNF TGA curves due to the evaporation of absorbed and intermolecular H-bonded water (Mu et al. 2012). The degradation temperature of oxidized CNF is obviously reduced when compared with CNF. The T_{20} (weight loss of 20%) of CNF is 323.2 °C, which is higher than T_{20} of CNF-1, CNF-2, CNF-3 and CNF-4 (310.9 °C, 291.6 °C, 259.1 °C and 248.0 °C). The decrease in thermal performance is caused by the reduction of hydrogen bond after the oxidation of CNF (Cui et al. 2014).

The crystallinity of cellulose after oxidation has undergone tremendous changes. The DTA results also indicate that the crystal structure of CNF has changed. The cellulose crystallization endothermic peaks slightly shift from 80 to 88 °C with increasing the $NaIO_4$ content. Moreover, the temperature at the maximum decomposition endothermic peak of CNF, CNF-1, CNF-2 slowly decrease with increasing the oxidant content. In contrast, CNF-3 and CNF-4 only have the weak decomposition endothermic peak at 227.2 and 188.5 °C, the decomposition process is basically a continuous exothermic state (Fig. 4). This result indicates that the high oxidation degree disrupts intramolecular hydrogen bonds and intermolecular hydrogen bonds of CNF, resulting in a significant decrease in the thermal performance of CNF.

Morphology of oxidation CNF

SEM was utilized to examine the morphology of CNF and oxidized CNF. The purchased commercial CNF shows that the diameter of cellulose nanofibers in the range of 50–500 nm (Fig. 5a). The diameter of CNF greatly changed when a certain amount of $NaIO_4$ is added to the CNF suspension. It is observed that the diameter of oxidized CNF is increased to 100–500 nm by adding 0.25 g $NaIO_4$ (Fig. 5b). When more oxidants are added, the oxidized CNF with a diameter of less than 200 nm is gradually disappeared (Fig. 5c–e). The phenomenon indicates that as the oxidant content increases, a large number of hydrogen bonds between the cellulose molecules are ruptured, resulting in more aldehyde CNF macromolecules being dissolved in aqueous solution. The low-diameter CNF is more susceptible to oxidation and dissolution, therefore, the remaining aldehyde CNF shows a large diameter after centrifugation. As the diameter of the oxidized CNF increases and the hydrophilicity of the oxidized CNF decreases (C–OH group converts into –CHO on the surface of CNF), the stability of the oxidized CNF in water has changed. The stability of CNF in water decreased with more $NaIO_4$ added, after 7 days of sedimentation experiment (Fig. 6).

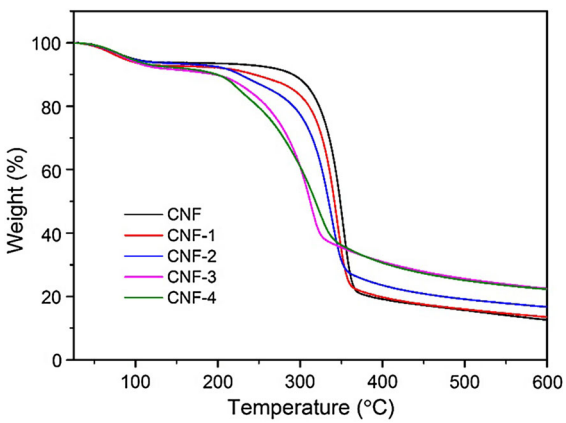

Fig. 3 TGA curves of CNF and oxidized CNF

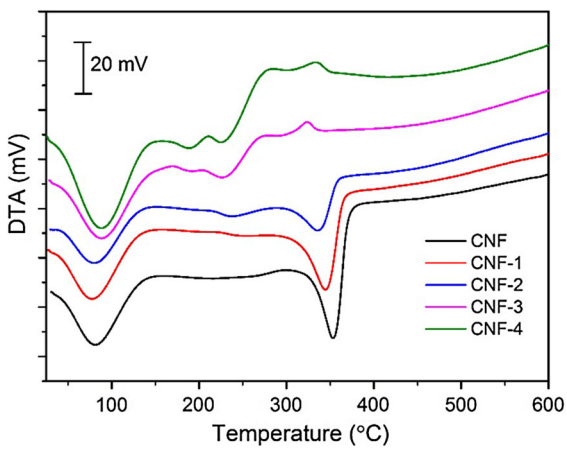

Fig. 4 DTA curves of CNF and oxidized CNF

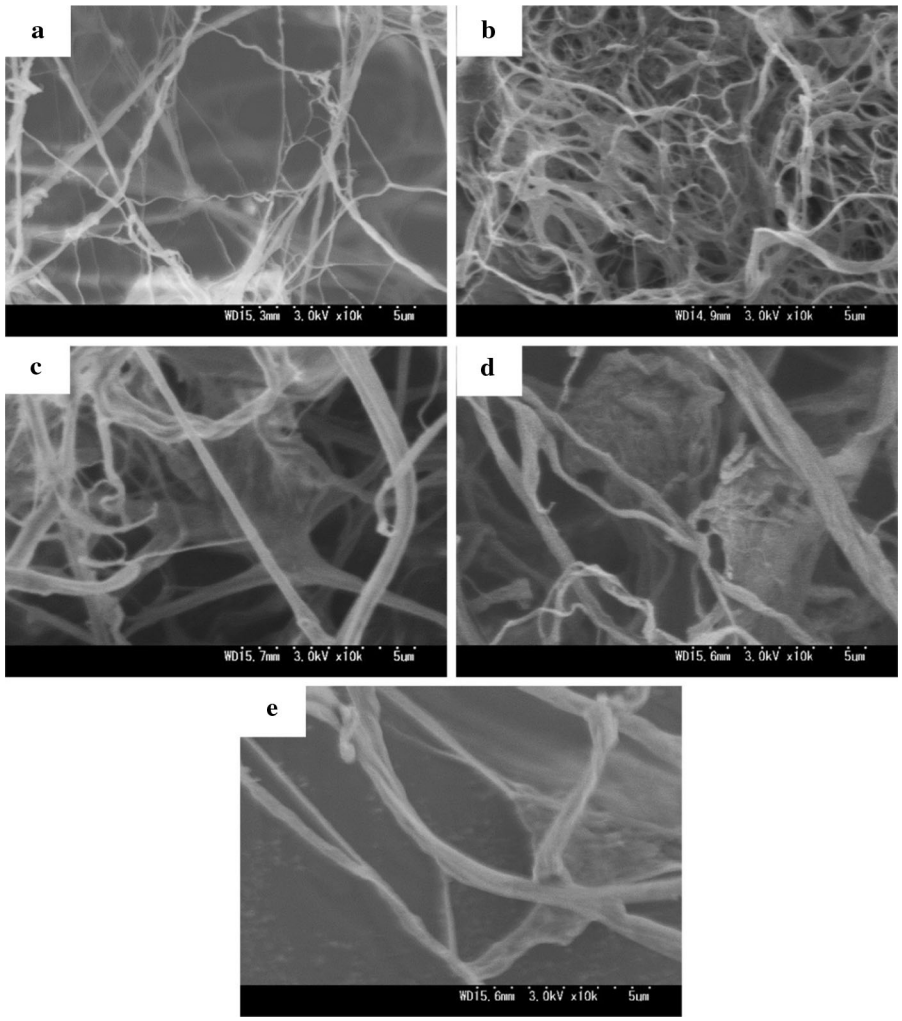

Fig. 5 SEM images of CNF and oxidized CNF. **a** CNF, **b** CNF-1, **c** CNF-2, **d** CNF-3, **e** CNF-4

Synthesis of hydrogel

The reactivity of the CNF is greatly improved after the introduction of the aldehyde group on the surface of CNF. The CNF with multiple aldehydes can be used as a natural macromolecule cross-linker. For example, Ragauskas et al. reported a biocompatible gelatin hydrogel with oxidized cellulose nanowhiskers as cross-linker (Dash et al. 2013). Although the preparation of the hydrogel is very gentle, the degree of chemical cross-linking between gelatin and nanowhiskers can be as high as 0.14–17%. In the present study, CNF/PVA hydrogels were prepared by aldolization with aldehyde CNF and PVA under acid catalysis at 80 °C. The color of obtained hydrogels (CNF-1/PVA to CNF-4/PVA) turned from light yellow to yellow. For comparison, the raw CNF and PVA mixture has no chemical reaction (Fig. 7). It should be noticed that although the CNF-1 and PVA mixture have aldolization, the resulting product does not form a hydrogel. This may be due to the small number of aldehyde groups on the surface of CNF-1, making CNF-1 and PVA difficult to generate enough cross-linked sites to form a hydrogel.

In the spectrum of CNF-3, the peaks around 3370 cm^{-1} and 2900 cm^{-1} are attributed to the stretching vibration of O–H and C–H, respectively. The peaks at 1115 cm^{-1} and 1160 cm^{-1} are absorption peaks of C–OH and C–C, respectively. Due to their high hydrophilicity, CNF or PVA will adsorb a

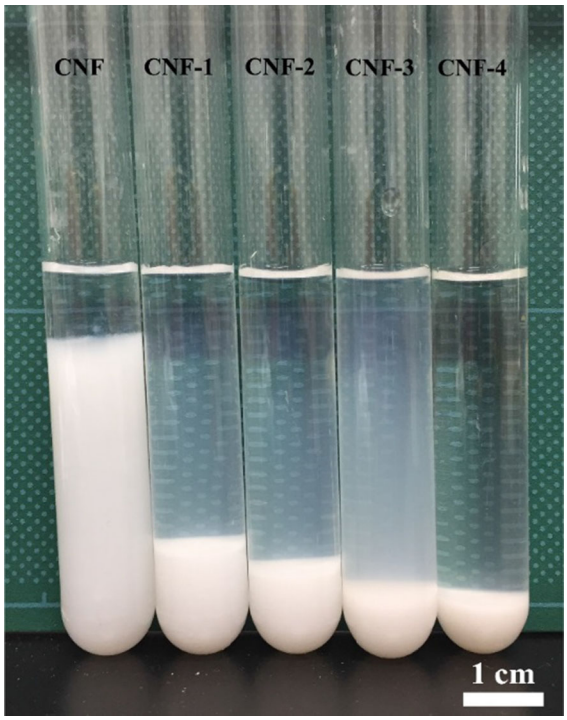

Fig. 6 Digital image of 0.15 wt % CNF and oxidized CNF suspension after settlement for 7 days

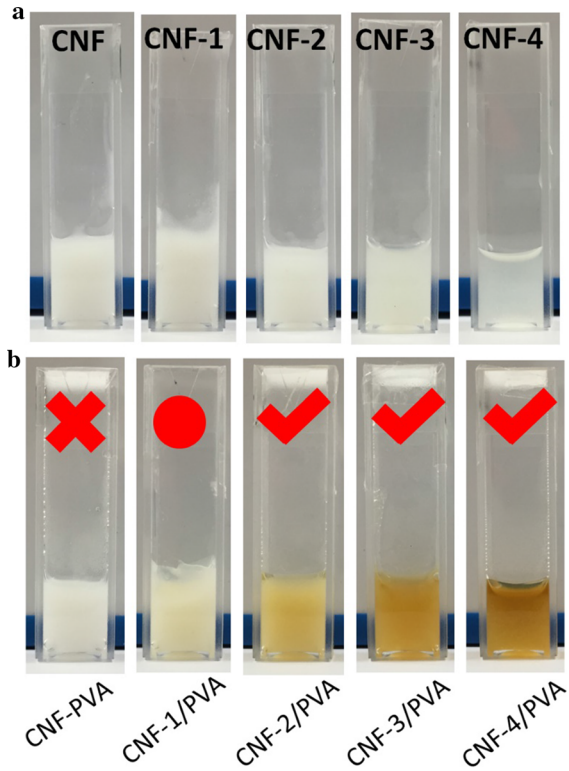

Fig. 7 Digital images of CNF and PVA mixture **a** before and **b** after aldolization

small amount of water during the FT-IR samples preparation. Therefore, the peak at 1635 cm^{-1} or 1650 cm^{-1} is the absorption peak of water (Peresin et al. 2010). Since PVA contains incompletely hydrolyzed ester groups, there are significant absorption peaks at 1714, 1568 and 1143 cm^{-1}. During the gelation reaction, the ester groups in the PVA were hydrolyzed due to the presence of the acid catalyst, and the absorption peaks at 1714 and 1568 cm^{-1} disappeared. After the aldolization, the absorption peak of CNF-3/PVA at 1143 cm^{-1} was lower than that of PVA. This is because part of the PVA cross-links with CNF-3, hindering the formation of C–OH (PVA) crystals in the hydrogel (Mallapragada and Peppas 1996). Moreover, the peak at 1085–1150 cm^{-1} is the absorption peak of C–O–C (Mansur et al. 2008).The absorption intensity of CNF-3/PVA is higher than that of PVA at 1085–1150 cm^{-1}, indicating that C–O–C is formed in the hydrogel by aldolization (Fig. 8).

Mechanical properties of hydrogel

In previous work, the E–S method is an efficient way to enhance the mechanical properties of hydrogels (Zhu et al. 2017a). This convenient method uses the hydrogen bond reconstruction to reinforce the mechanical properties of the hydrogel. The CNF-PVA, CNF-1/PVA and synthesized hydrogel (CNF-2/PVA, CNF-3/PVA and CNF-4/PVA) are further strengthened through E-S method. This convenient method enables the non-cross-linked mixture (CNF-PVA, CNF-1/PVA) to be a hydrogel. The tensile property of produced hydrogel is shown in Fig. 9. The hydrogel formed by the mixture of CNF and PVA had a tensile strength of 1.49 MPa, an fracture elongation of 180% and an elastic modulus of 1.54 MPa after treatment with E-S method. Similarly, CNF-1 and PVA also formed a tough hydrogel (tensile strength: 3.13 MPa, fracture elongation: 170%, elastic modulus: 2.10 MPa). The other three samples (CNF-2/PVA, CNF-3/PVA, and CNF-4/PVA) that have been gelled possess lower mechanical properties than the un-gelled hydrogel (CNF-1/PVA). The tensile strength and elastic modulus of CNF-2/PVA, CNF-3/PVA and CNF-4/PVA are range from 0.25 to 0.96 MPa and 0.14 to 0.42 MPa, respectively. This phenomenon may be

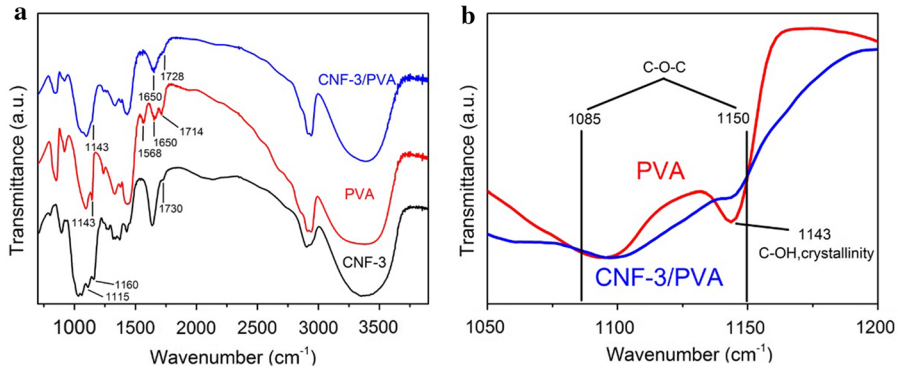

Fig. 8 **a** FT-IR spectra of CNF-3, PVA, and CNF-3/PVA. **b** Amplification image of **a**

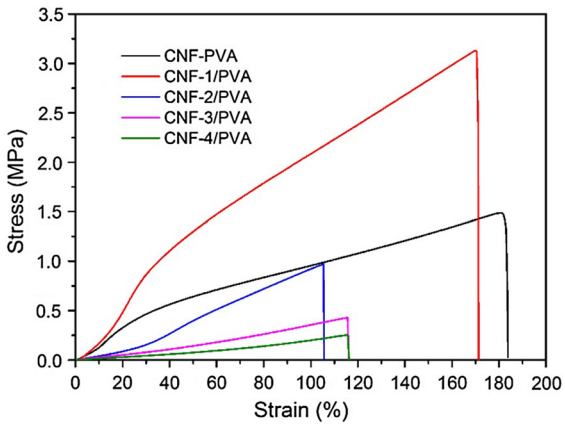

Fig. 9 Stress–strain curves of reinforced CNF/PVA hydrogel

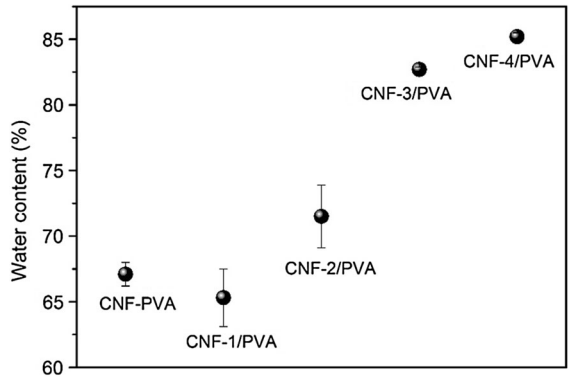

Fig. 11 Water content of reinforced CNF/PVA hydrogel

explained by the abundant chemical cross-linking sites limit the formation of hydrogen bonds of the hydrogel during the E–S process.

The reinforced hydrogel can undergo large compressive strains without damage. However, most hydrogels with hydrogen bonds or/and ionic cross-linking sites generally show the softening effect (also known as Mullins effect Diani et al. 2009) under cyclic large deformations (Webber et al. 2007). The softening effect is also found in natural living tissues which possess a similar composition with hydrogel (Peña et al. 2010). Figure 10a shows that the initial compressive strength of CNF-3/PVA hydrogel can reach 1.7 MPa at a strain of 70%.

With increasing the cyclic times the compressive stress gradually decreases, indicating that CNF-3/PVA hydrogel has softening effect. The softening ratio (SR) is calculated according to the modified equation (Chen et al. 2016):

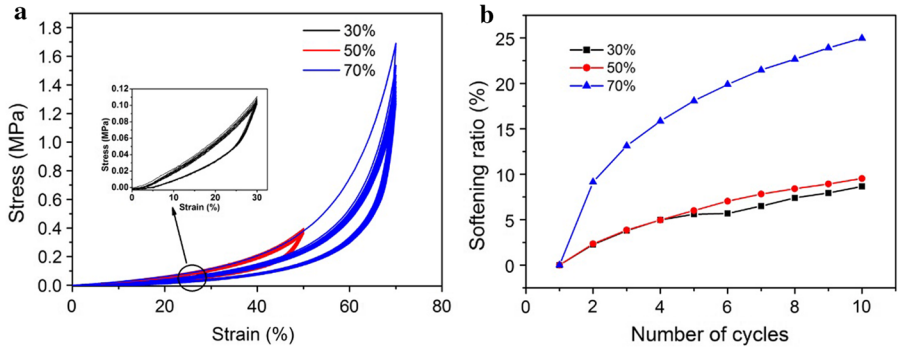

Fig. 10 **a** Cyclic compressive curves of CNF-3/PVA hydrogel obtained after 10 tests at various strains. **b** Softening ratio of CNF-3/PVA hydrogel at various strains

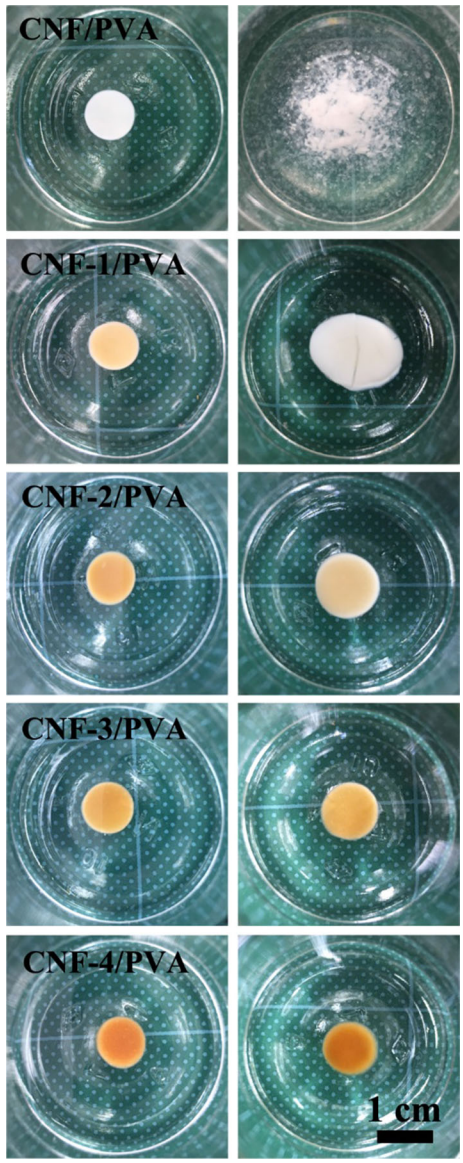

Fig. 12 Thermal property of CNF/PVA hydrogel before and after high temperature treatment

$$\mathrm{SR}\% = \frac{\sigma_n - \sigma_1}{\sigma_1} \times 100\% \quad (2)$$

where σ_1 represents the maximum stress at the first cycle; σ_n represents the maximum stress at the current cycle. At compressive strains of 30% and 50%, the softening ratios of the hydrogel are less than 10% and gradually tends to be a plateau. However, the softening rate of the hydrogel reaches 25% after 10 times of cyclic compression at 70% of the compressive strain (Fig. 10b). It indicated that when the compression strain is less than 50%, the internal network structure of the hydrogel changes slightly. On the contrary, the softening effect may be caused by sliding and disentanglement of polymer chains, and the rupture of hydrogen bonds and chemical bonds under large deformation (Zhu et al. 2017c).

Morphology of CNF/PVA hydrogel

The water content of the hydrogel is inversely proportional to the cross-linking density (Akar et al. 2012; Zhu et al. 2017b). Therefore, the water content of the CNF/PVA hydrogel after swelling equilibrium can reflect the state of the cross-linking network. As shown in Fig. 11, the water content increase from CNF-1/PVA to CNF-4/PVA, indicating that the density of the cross-linked network inside the hydrogel gradually decreases. The experimental data show that the un-cross-linked mixture (CNF/PVA and CNF-1/PVA) can obtain better mechanical properties than the chemical cross-linked hydrogel (CNF-2/PVA, CNF-3/PVA, and CNF-4/PVA) by the E-S method. However, the water contents of CNF/PVA and CNF-1/PVA (65.3% and 75.1%, respectively) are obviously lower than that of the soft tissue in the organism. As a tissue engineering material, the mechanical properties of CNF-2/PVA, CNF-3/PVA, and CNF-4/PVA are closer to the soft tissue properties of the organism. The hydrogel cross-linked only through hydrogen bonds is directly decomposed during the use of conventional high temperature autoclaving process (Fig. 12). In contrast, hydrogels (CNF-1/PVA, CNF-2/PVA) with low chemical cross-linking density did not decompose, but exhibit significant swelling; hydrogels (CNF-3/PVA, CNF-4/PVA) with high chemical cross-linking density show no significant change in morphology and water content. It is worth noting that after high temperature autoclaving process, the tensile strength of CNF-3/PVA and CNF-4/PVA are partially reduced, which may be due to the rupture of hydrogen bonds inside the hydrogel (Supporting information 1). This suggests that the chemically cross-linked hydrogel with aldehyde CNF as cross-linker has excellent high-temperature thermal stability, and can be conveniently processed using high-temperature sterilization before use.

The prepared hydrogels generally show porous network structure after the freeze-drying process (Fang et al. 2013). To investigate the microstructure

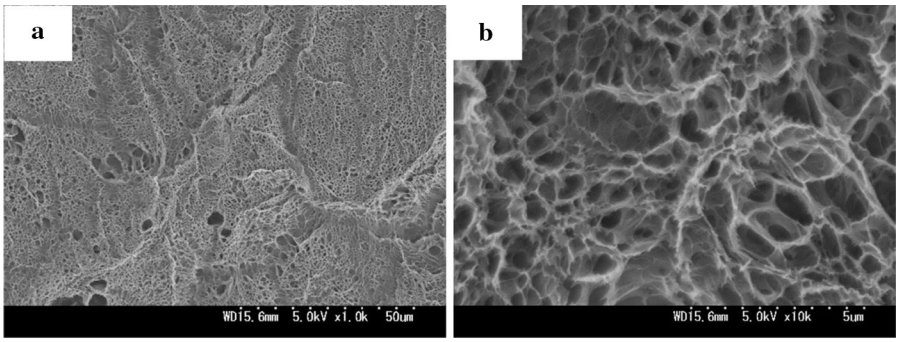

Fig. 13 **a** SEM images of CNF-3/PVA hydrogel. **b** Amplification image of **a**

of CNF/PVA hydrogel, SEM is utilized to observe the structure. The reinforced CNF-3/PVA hydrogel exhibits a porous network structure with the size of the porous is approximately 1 μm (Fig. 13a, b). No separate CNF is found in the SEM image, indicating that the CNF and PVA are completely fused together.

Conclusion

In this study, a novel high temperature resistant CNF/PVA hydrogel is synthesized by using multi-aldehyde CNF as chemical cross-linker. The CNF is first oxidized to the multi-aldehyde CNF using $NaIO_4$ as an oxidant. The crystallinity and decomposition temperature of the oxidized CNF decrease with increasing the amount of $NaIO_4$. The CNF/PVA hydrogels are prepared with aldehyde CNF and PVA at 80 °C under acidic condition through aldolization. Hydrogels containing more chemical cross-linking sites can effectively reduce the formation of hydrogen-bonding networks within the hydrogel when the hydrogel is reinforced with the E–S method. The tensile strength and elastic modulus of CNF-3/PVA prepared with more chemical cross-linking networks are 0.43 MPa and 0.25 MPa, respectively. The wet and soft hydrogel (CNF-3/PVA) has an ideal water content (82.7%) and a softening effect closer to the natural soft tissues, and exhibits thermal stability during conventional high temperature autoclaving process.

Acknowledgments This research was supported by the Natural Science Foundation of Shandong Province, China (ZR2019BEM035). J. Qiu are grateful to the financial supports from Shenzhen Government Foundation Project (JCYJ20160331185322137).

References

Abitbol T, Johnstone T, Quinn TM, Gray DG (2011) Reinforcement with cellulose nanocrystals of poly(vinyl alcohol) hydrogels prepared by cyclic freezing and thawing. Soft Matter 7:2373–2379. https://doi.org/10.1039/c0sm01172j

Akar E, Altinisik A, Seki Y (2012) Preparation of pH- and ionic-strength responsive biodegradable fumaric acid crosslinked carboxymethyl cellulose. Carbohydr Polym 90:1634–1641. https://doi.org/10.1016/j.carbpol.2012.07.043

Baker MI, Walsh SP, Schwartz Z, Boyan BD (2012) A review of polyvinyl alcohol and its uses in cartilage and orthopedic applications. J Biomed Mater Res B 100:1451–1457. https://doi.org/10.1002/jbm.b.32694

Battirola LC, Andrade PF, Marson GV, Hubinger MD, do Carmo Gonçalves M (2017) Cellulose acetate/cellulose nanofiber membranes for whey and fruit juice microfiltration. Cellulose 24:5593–5604. https://doi.org/10.1007/s10570-017-1510-8

Chen Q, Chen H, Zhu L, Zheng J (2015) Fundamentals of double network hydrogels. J Mater Chem B 3:3654–3676. https://doi.org/10.1039/c5tb00123d

Chen G, Zhang Y, Xu D, Lin Y, Chen X (2016) Low cycle fatigue and creep-fatigue interaction behavior of nickel-base superalloy GH4169 at elevated temperature of 650 °C. Mater Sci Eng, A 655:175–182. https://doi.org/10.1016/j.msea.2015.12.096

Chin SY, Poh YC, Kohler A-C, Compton JT, Hsu LL, Lau KM, Kim S, Lee BW, Lee FY, Sia SK (2017) Additive manufacturing of hydrogel-based materials for next-generation implantable medical devices. Sci Robot 2:eaah6451. https://doi.org/10.1126/scirobotics.aah6451

Cui Q, Zheng Y, Lin Q, Song W, Qiao K, Liu S (2014) Selective oxidation of bacterial cellulose by NO_2–HNO_3. RSC Adv 4(4):1630–1639

Dash R, Foston M, Ragauskas AJ (2013) Improving the mechanical and thermal properties of gelatin hydrogels cross-linked by cellulose nanowhiskers. Carbohyd Polym 91:638–645. https://doi.org/10.1016/j.carbpol.2012.08.080

Diani J, Fayolle B, Gilormini P (2009) A review on the Mullins effect. Eur Polym J 45:601–612. https://doi.org/10.1016/j.eurpolymj.2008.11.017

Dong D, Li J, Cui M, Wang J, Zhou Y, Luo L, Wei Y, Ye L, Sun H, Yao F (2016) In situ "clickable" zwitterionic starch-based hydrogel for 3D cell encapsulation. ACS Appl Mater Inter 8:4442–4455. https://doi.org/10.1021/acsami.5b12141

Elsner JJ, Berdicevsky I, Zilberman M (2011) In vitro microbial inhibition and cellular response to novel biodegradable composite wound dressings with controlled release of antibiotics. Acta Biomater 7:325–336. https://doi.org/10.1016/j.actbio.2010.07.013

Fang J, Mehlich A, Koga N, Huang J, Koga R, Gao X, Hu C, Jin C, Rief M, Kast J, Baker D, Li H (2013) Forced protein unfolding leads to highly elastic and tough protein hydrogels. Nat Commun 4:2974. https://doi.org/10.1038/ncomms3974

French AD (2014) Idealized powder diffraction patterns for cellulose polymorphs. Cellulose 21(2):885–896. https://doi.org/10.1007/s10570-013-0030-4

French AD (2017) Glucose, not cellobiose, is the repeating unit of cellulose and why that is important. Cellulose 24(11):4605–4609. https://doi.org/10.1007/s10570-017-1450-3

Gong JP (2010) Why are double network hydrogels so tough? Soft Matter 6:2583. https://doi.org/10.1039/b924290b

Hoffman AS (2012) Hydrogels for biomedical applications. Adv Drug Deliv Rev 64:18–23. https://doi.org/10.1016/j.addr.2012.09.010

Kamoun EA, Kenawy ES, Chen X (2017) A review on polymeric hydrogel membranes for wound dressing applications: PVA-based hydrogel dressings. J Adv Res 8:217–233. https://doi.org/10.1016/j.jare.2017.01.005

Karlgard C, Wong N, Jones L, Moresoli C (2003) In vitro uptake and release studies of ocular pharmaceutical agents by silicon-containing and p-HEMA hydrogel contact lens materials. Int J Pharmaceut 257:141–151. https://doi.org/10.1016/S0378-5173(03)00124-8

Kim U-J, Wada M, Kuga S (2004) Solubilization of dialdehyde cellulose by hot water. Carbohydr Polym 56:7–10. https://doi.org/10.1016/j.carbpol.2003.10.013

Kim J, Conway A, Chauhan A (2008) Extended delivery of ophthalmic drugs by silicone hydrogel contact lenses. Biomaterials 29:2259–2269. https://doi.org/10.1016/j.biomaterials.2008.01.030

Klemm D, Kramer F, Moritz S, Lindstrom T, Ankerfors M, Gray D, Dorris A (2011) Nanocelluloses: a new family of nature-based materials. Angew Chem Int Edit 50:5438–5466. https://doi.org/10.1002/anie.201001273

Krumova M, López D, Benavente R, Mijangos C, Pereña JM (2000) Effect of crosslinking on the mechanical and thermal properties of poly(vinyl alcohol). Polymer 41:9265–9272. https://doi.org/10.1016/s0032-3861(00)00287-1

Lin N, Dufresne A (2014) Nanocellulose in biomedicine: current status and future prospect. Eur Polym J 59:302–325. https://doi.org/10.1016/j.eurpolymj.2014.07.025

Mallapragada SK, Peppas NA (1996) Dissolution mechanism of semicrystalline poly(vinyl alcohol) in water. J Polym Sci Pol Phys 34:1339–1346. https://doi.org/10.1002/(SICI)1099-0488(199605)34:7%3c1339:AID-POLB15%3e3.0.CO;2-B

Mansur HS, Sadahira CM, Souza AN, Mansur AA (2008) FTIR spectroscopy characterization of poly(vinyl alcohol) hydrogel with different hydrolysis degree and chemically crosslinked with glutaraldehyde. Mater Sci Eng, C 28:539–548. https://doi.org/10.1016/j.msec.2007.10.088

Mu C, Guo J, Li X, Lin W, Li D (2012) Preparation and properties of dialdehyde carboxymethyl cellulose crosslinked gelatin edible films. Food Hydrocoll 27:22–29. https://doi.org/10.1016/j.foodhyd.2011.09.005

Peña E, Alastrué V, Laborda A, Martínez MA, Doblaré M (2010) A constitutive formulation of vascular tissue mechanics including viscoelasticity and softening behaviour. J Biomech 43:984–989. https://doi.org/10.1016/j.jbiomech.2009.10.046

Peppas NA, Merrill EW (1976) Differential scanning calorimetry of crystallized PVA hydrogels. J Appl Polym Sci 20:1457–1465. https://doi.org/10.1002/app.1976.070200604

Peresin MS, Habibi Y, Zoppe JO, Pawlak JJ, Rojas OJ (2010) Nanofiber composites of polyvinyl alcohol and cellulose nanocrystals: manufacture and characterization. Biomacromol 11:674–681. https://doi.org/10.1021/bm901254n

Qi Y, Min H, Mujeeb A, Zhang Y, Han X, Zhao X, Anderson GJ, Zhao Y, Nie G (2018) Injectable hexapeptide hydrogel for localized chemotherapy prevents breast cancer recurrence. ACS Appl Mater Inter 10:6972–6981. https://doi.org/10.1021/acsami.7b19258

Ramaraj B (2007) Crosslinked poly(vinyl alcohol) and starch composite films. II. Physicomechanical, thermal properties and swelling studies. J Appl Polym Sci 103:909–916. https://doi.org/10.1002/app.25237

Shi Y, Xiong D (2013) Microstructure and friction properties of PVA/PVP hydrogels for articular cartilage repair as function of polymerization degree and polymer concentration. Wear 305:280–285. https://doi.org/10.1016/j.wear.2012.12.020

Slaughter BV, Khurshid SS, Fisher OZ, Khademhosseini A, Peppas NA (2009) Hydrogels in regenerative medicine. Adv Mater 21:3307–3329. https://doi.org/10.1002/adma.200802106

Thygesen A, Oddershede J, Lilholt H, Thomsen AB, Ståhl K (2005) On the determination of crystallinity and cellulose content in plant fibres. Cellulose 12:563. https://doi.org/10.1007/s10570-005-9001-8

Tubbs RK (1966) Sequence distribution of partially hydrolyzed poly(vinyl acetate). J Polym Sci Pol Chem 4:623–629. https://doi.org/10.1002/pol.1966.150040316

Tummala GK, Joffre T, Lopes VR, Liszka A, Buznyk O, Ferraz N, Persson C, Griffith M, Mihranyan A (2016a) Hyperelastic nanocellulose-reinforced hydrogel of high water content for ophthalmic applications. ACS Biomater Sci Eng 2:2072–2079. https://doi.org/10.1021/acsbiomaterials.6b00484

Tummala GK, Rojas R, Mihranyan A (2016b) Poly(vinyl alcohol) hydrogels reinforced with nanocellulose for ophthalmic applications: general characteristics and optical properties. J Phys Chem B 120:13094–13101. https://doi.org/10.1021/acs.jpcb.6b10650

Tummala GK, Joffre T, Rojas R, Persson C, Mihranyan A (2017) Strain-induced stiffening of nanocellulose-reinforced poly(vinyl alcohol) hydrogels mimicking collagenous soft tissues. Soft Matter 13:3936–3945. https://doi.org/10.1039/c7sm00677b

Webber RE, Creton C, Brown HR, Gong JP (2007) Large strain hysteresis and mullins effect of tough double-network

hydrogels. Macromolecules 40:2919–2927. https://doi.org/10.1021/ma062924y

Yang X, Abe K, Biswas SK, Yano H (2018) Extremely stiff and strong nanocomposite hydrogels with stretchable cellulose nanofiber/poly(vinyl alcohol) networks. Cellulose 25:6571–6580. https://doi.org/10.1007/s10570-018-2030-x

Zhang X-F, Feng Y, Huang C, Pan Y, Yao J (2017) Temperature-induced formation of cellulose nanofiber film with remarkably high gas separation performance. Cellulose 24:5649–5656. https://doi.org/10.1007/s10570-017-1529-x

Zhu L, Qiu J, Sakai E (2017a) A high modulus hydrogel obtained from hydrogen bond reconstruction and its application in vibration damper. RSC Adv 7:43755–43763. https://doi.org/10.1039/c7ra08272j

Zhu L, Qiu J, Sakai E, Ito K (2017b) Rapid recovery double cross-linking hydrogel with stable mechanical properties and high resilience triggered by visible light. ACS Appl Mater Inter 9:13593–13601. https://doi.org/10.1021/acsami.7b01003

Zhu L, Qiu J, Sakai E, Zang L, Yu Y, Ito K, Liu P, Kang F (2017c) Design of a rubbery carboxymethyl cellulose/polyacrylic acid hydrogel via visible-light-triggered polymerization. Macromol Mater Eng 302(6):1600509. https://doi.org/10.1002/mame.201600509